



Effective and efficient algorithm for the Wigner rotation matrix at high angular momenta

Bin-Lei Wang, Fan Gao, and Long-Jun Wang 

School of Physical Science and Technology, Southwest University, Chongqing 400715, China

Yang Sun 

School of Physics and Astronomy, Shanghai Jiao Tong University, Shanghai 200240, China



(Received 29 July 2022; accepted 20 October 2022; published 16 November 2022)

The Wigner rotation matrix (d function), which appears as a part of the angular-momentum-projection operator, plays a crucial role in modern nuclear-structure models. However, it is a longstanding problem that its numerical evaluation suffers from serious errors and instability, which hinders precise calculations for nuclear high-spin states. Recently, Tajima [Phys. Rev. C **91**, 014320 (2015)] has made a significant step toward solving the problem by suggesting the high-precision Fourier method, which however relies on formula-manipulation softwares. In this paper we propose an effective and efficient algorithm for the Wigner d function based on the Jacobi polynomials. We compare our method with the conventional Wigner method and the Tajima Fourier method through some testing calculations, and demonstrate that our algorithm can always give stable results with similar high-precision as the Fourier method, and in some cases (for special sets of j , m , k , and θ) ours are even more accurate. Moreover, our method is self-contained and less memory consuming. By taking the ^{156}Dy yrast band as an example, we show that with the d function calculated by our proposed Jacobi method in the angular-momentum projector, the realistic projected-shell-model calculation can be aggressively extended to the high-spin region where the conventional Wigner method collapses completely. A related testing code and subroutines for the three algorithms of d function are provided as Supplemental Material in the present paper.

DOI: [10.1103/PhysRevC.106.054320](https://doi.org/10.1103/PhysRevC.106.054320)

I. INTRODUCTION

The microscopic description of collective rotational motion involves quantum-mechanical treatment of angular momentum, in which the three angular-momentum operators, \hat{j}_i ($i = x, y, z$), are generators of the Lie algebra of SU(2) and SO(3). The Wigner D matrix, a unitary matrix in an irreducible representation of the groups SU(2) and SO(3), enters into the discussion when functions of angular momentum are transformed by the rotation operator $\hat{R}(\phi, \theta, \psi) = e^{-i\phi\hat{j}_z} e^{-i\theta\hat{j}_y} e^{-i\psi\hat{j}_z}$ with the Euler angles (ϕ, θ, ψ) [1]. If the eigenstates of the angular momentum operators are expressed in the spherical basis and labeled by the quantum number j (with $j = 0, \frac{1}{2}, 1, \frac{3}{2}, \dots$) and the projection on the z axis with $2j + 1$ quantum numbers labeled as m or $k = -j, -j + 1, \dots, j - 1, j$, the Wigner D matrix can be written as

$$\begin{aligned} D_{mk}^j(\phi, \theta, \psi) &= \langle jm | e^{-i\phi\hat{j}_z} e^{-i\theta\hat{j}_y} e^{-i\psi\hat{j}_z} | jk \rangle \\ &= e^{-i(m\phi+k\psi)} d_{mk}^j(\theta), \end{aligned} \quad (1)$$

where

$$d_{mk}^j(\theta) = \langle jm | e^{-i\theta\hat{j}_y} | jk \rangle \quad (2)$$

is the key part in the expression, referred to as Wigner (small) d matrix. As Eqs. (1) and (2) are functions of the Euler

angles for different sets of quantum numbers $\{j, m, k\}$, they are usually called Wigner D (d) functions, respectively [2,3].

As its characteristic feature, $d_{mk}^j(\theta)$ is known as an oscillation function of θ . In general, the oscillation frequency of the d function increases rapidly with the angular momentum j . Figure 1 shows the example for $j = 30\hbar$.

The Wigner D function plays crucial roles in many discussions of modern physics. As a set of orthogonal functions of the Euler angles, the D function can be used to expand other functions. The D function is related to some other well-known functions, as for instance, $D_{m0}^j(\phi, \theta, \psi) = \sqrt{\frac{4\pi}{2j+1}} Y_{jm}^*(\theta, \phi)$ and $D_{00}^j(\phi, \theta, \psi) = P_j(\cos \theta)$, where Y_{jm} (P_j) is the spherical harmonic function (Legendre polynomial) [2,4]. Furthermore, irreducible tensors can be well defined with the help of the Wigner D function. Therefore, the Wigner D function is indispensable in the study of modern physics, for example in nuclear physics [5], quantum metrology [6,7], and many other fields [8,9]. Especially in theoretical calculations with the nuclear beyond-mean-field methods [10–16], where angular-momentum projection serves as an important ingredient, the Wigner D function is the central part of the angular-momentum projector [10,17–27]. Angular-momentum projected wave functions obtained in modern nuclear theories are applied to the study of β decay [28,29], neutrinoless double- β decay [30–32], astrophysical weak process [33–35], nuclear fission [36–40], and many others.

All the above applications require a numerically accurate and computationally stable evaluation of the small d function.

*longjun@swu.edu.cn

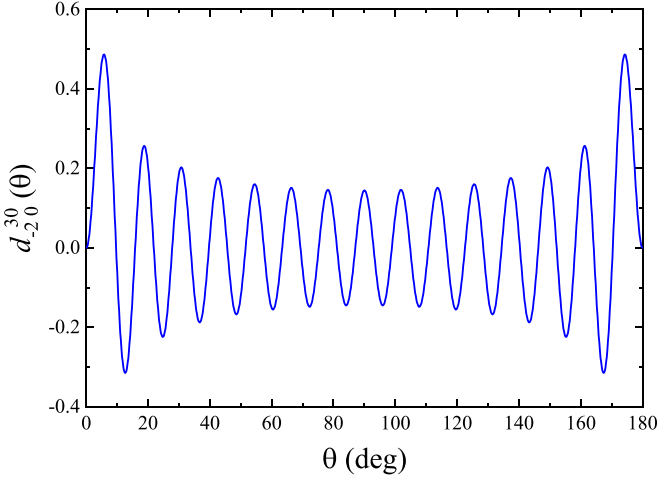


FIG. 1. The highly oscillatory behavior of the Wigner $d_{mk}^j(\theta)$ function with $j = 30$, $m = -2$, $k = 0$.

However, due to the presence of many factorials of large numbers in the formula [2,41], numerical calculations of the d function by the conventional Wigner method suffers from a serious loss of precision at medium and high spins. Although a few remedies have been proposed [42–44], they still encounters severe numerical instability and/or loss of precision from unclear sources. A few years ago, Tajima [3] proposed a new method for the Wigner d -function evaluation based on the Fourier-series expansion. In this method, the precision of the d function is determined by accurate evaluation of the Fourier coefficients. This method turns out to be of a significant improvement for the numerical stability and precision in the d -function evaluation. However, those Fourier coefficients still involve many factorials of large numbers so that they have to be evaluated with the assistance of a formula-manipulation software. Besides, those Fourier coefficients take up a lot of memory in the numerical procedure.

In this work, we propose an alternative method based on the Jacobi polynomials with a stable and high-precision algorithm for the Wigner d -function evaluation. We show that our method can achieve a very similar precision and stable result as the Tajima Fourier method, but ours may be more efficient and user-friendly. In Sec. II we provide, step by step, the analytic expressions of the Wigner, Fourier, and Jacobi methods for the Wigner d function. The precision of the Jacobi method is analyzed in details and compared with both the Wigner and Fourier methods in Secs. III and IV. A realistic calculation of high-spin states for ^{156}Dy by different d -function methods is discussed in Sec. V, and we finally summarize our work in Sec. VI.

II. DIFFERENT METHODS FOR THE WIGNER d -FUNCTION EVALUATION

The conventional method for the d function is based on the following Wigner formula [2], i.e.:

$$d_{mk}^j(\theta) = \sum_{n=n_{\min}}^{n_{\max}} (-1)^n W_n^{jmk}(\theta), \quad (3)$$

where

$$n_{\min} = \max(0, k - m), \quad (4a)$$

$$n_{\max} = \min(j - m, j + k), \quad (4b)$$

and

$$W_n^{jmk}(\theta) = w_n^{jmk} \left(\cos \frac{\theta}{2} \right)^{2j+k-m-2n} \left(-\sin \frac{\theta}{2} \right)^{m-k+2n} \quad (5)$$

with

$$w_n^{jmk} = \frac{\sqrt{(j+m)!(j-m)!(j+k)!(j-k)!}}{(j-m-n)!(j+k-n)!(n+m-k)!n!}. \quad (6)$$

It can be seen that the Wigner formula (3) involves a summation over many terms, W_n^{jmk} , with alternating signs. Each of these terms includes many factorials of large numbers, especially at medium and high spins, as they grow exponentially with j ($W_n^{jmk} \approx 2^j$). Although cancellation among these terms should finally lead the summation to a normal value for the d function, the procedure would however cause an accumulation of numerical errors. Thus the numerical results from the Wigner formula unavoidably suffers from a serious loss of precision at medium and high spins, except for the neighborhood of $\theta = 0$ and π [3].

The problem is the repeated production and cancellation of large numbers. To avoid the problem, Tajima [3] proposed a new method for the Wigner d function based on Fourier-series expansion, in which the d function can be expressed as

$$d_{mk}^j(\theta) = \sum_{\rho=\rho_{\min}}^j t_{\rho}^{jmk} f(\rho\theta). \quad (7)$$

In the above formula, ρ_{\min} could be 0, 1/2, or 1 depending on the values of j , m , and k (see Table I of Ref. [3] for details) and f is sin (cos) function for $m - k$ being odd (even). In Eq. (7) the Fourier coefficient reads

$$t_{\rho}^{jmk} = \frac{2(-1)^{m-k}}{1 + \delta_{\rho 0}} \sum_{n=n_{\min}}^{n_{\max}} (-1)^n w_n^{jmk} \sum_{r=0}^{\lfloor \rho - \frac{1}{2} \rfloor} (-1)^r \binom{2\rho}{2r+p} \times \frac{1}{2\pi} I_{2(j+\rho-n-r)-m+k-p, 2(n+r)+m-k+p}, \quad (8)$$

where $p \equiv |m - k| \pmod{2}$, the square brackets are the floor function [3], $\binom{\rho}{r} = \rho!/[r!(\rho - r)!]$, and

$$I_{\lambda,\alpha} = \int_0^{2\pi} \cos^{\lambda} x \sin^{\alpha} x dx. \quad (9)$$

The Fourier method avoids cancellation among terms with large numbers since each Fourier coefficient, t_{ρ}^{jmk} , is less than or equal to 1. It has indeed much improved the calculation of the d function. However, two factors may limit its application. On one hand, the Fourier coefficient, t_{ρ}^{jmk} , still includes many factorials of large numbers, i.e., w_n^{jmk} , so that it has to be calculated by means of formula-manipulation software such as MAXIMA or Mathematica [3]. On the other hand, in practical applications, one has to read t_{ρ}^{jmk} from files and store into a

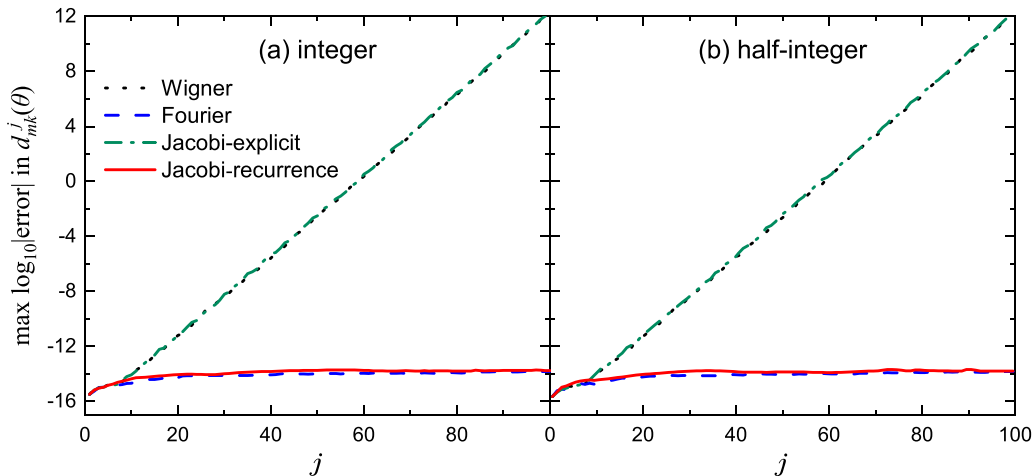


FIG. 2. The common logarithm of the maximum error in the numerical value of the d function $d_{mk}^j(\theta)$ as a function of j for both integer and half-integer cases of j , with the Wigner, Fourier, and Jacobi methods. The exact values of $d_{mk}^j(\theta)$ are obtained by *Mathematica 12.1* and the maximum error is taken over all the possible values of m , k , and θ for each j . See the text for details.

memory, which consumes about 70 MB (1.2 GB) space for the case of $j \leq 50$ ($j \leq 100$) [3]. Recently, Feng *et al.* put forward an exact-diagonalization method to calculate the Fourier coefficients, in which the corresponding precision of the d function decreases a little and the requested space doubles to be about 2.4 GB for the case of $j \leq 100$ [41].

It is thus desired to have an efficient algorithm for the d -function evaluation, which, while keeps the high precision as of the Tajima Fourier method, is self-contained, and therefore, user-friendly. Towards this goal, we note that the Wigner d function can be expressed in terms of the Jacobi polynomials [2]

$$d_{mk}^j(\theta) = \xi_{mk} \left[\frac{s!(s+\mu+\nu)!}{(s+\mu)!(s+\nu)!} \right]^{1/2} \times \left(\sin \frac{\theta}{2} \right)^\mu \left(\cos \frac{\theta}{2} \right)^\nu P_s^{(\mu,\nu)}(\cos \theta), \quad (10)$$

where $\mu = |m-k|$, $\nu = |m+k|$, $s = j - \frac{1}{2}(\mu+\nu)$, and

$$\xi_{mk} = \begin{cases} 1 & \text{if } k \geq m, \\ (-1)^{k-m} & \text{if } k < m. \end{cases} \quad (11)$$

The Jacobi polynomial in Eq. (10) can be calculated by its explicit expression [45]

$$P_s^{(\mu,\nu)}(z) = \frac{1}{2^s} \sum_{n=0}^s \binom{s+\mu}{n} \binom{s+\nu}{s-n} (z-1)^{s-n} (z+1)^n, \quad (12)$$

or by the corresponding recurrence relations [45]

$$\begin{aligned} & 2s(s+\mu+\nu)(2s+\mu+\nu-2)P_s^{(\mu,\nu)}(z) \\ &= (2s+\mu+\nu-1)[(2s+\mu+\nu)(2s+\mu+\nu-2)z \\ &+ \mu^2 - \nu^2]P_{s-1}^{(\mu,\nu)}(z) \\ &- 2(s+\mu-1)(s+\nu-1)(2s+\mu+\nu)P_{s-2}^{(\mu,\nu)}(z) \end{aligned} \quad (13)$$

with

$$P_0^{(\mu,\nu)}(z) = 1, \quad (14a)$$

$$P_1^{(\mu,\nu)}(z) = (\mu+1) + (\mu+\nu+2)\frac{z-1}{2}. \quad (14b)$$

It is important to realize that unlike the Wigner method and the Fourier method, the expression in Eq. (10) that leads to the Wigner d function does not involve a summation over many terms with large numbers.

III. ERROR ANALYSIS OF THE JACOBI METHOD

In this and the next sections we carry out error analysis and discuss precision of the Jacobi method in Eq. (10) by comparing with the conventional Wigner method and the recent Fourier method. In Figs. 2 and 3 the absolute errors for the d function from the three different methods are presented, and in Fig. 4 the errors in an integral calculation involving the d function are illustrated. All these results are obtained by a FORTRAN90 testing code with standard subroutines for the Wigner, Fourier, and Jacobi methods as provided in the Supplemental Material [46], where in all cases floating-point numbers are adopted as double-precision (64-bit) real number.

First in Fig. 2, we show maximum errors of the $d_{mk}^j(\theta)$ calculation as a function of j , obtained from the Wigner, Fourier, and Jacobi methods. Results for integer and half-integer j 's are illustrated separately. Each error of $d_{mk}^j(\theta)$ is evaluated with respect to the exact value calculated from the formula-manipulation software *Mathematica 12.1* where higher than 10^{-25} precision is kept. The maximum of the errors is recorded by considering all θ 's from 0° to 180° with an increment of 5° , and for all possible values of m and k with $0 \leq m \leq j$ and $k \leq |m|$ due to the following symmetries:

$$d_{mk}^j(\theta) = (-1)^{m-k} d_{-m-k}^j(\theta), \quad (15a)$$

$$d_{mk}^j(\theta) = (-1)^{m-k} d_{km}^j(\theta), \quad (15b)$$

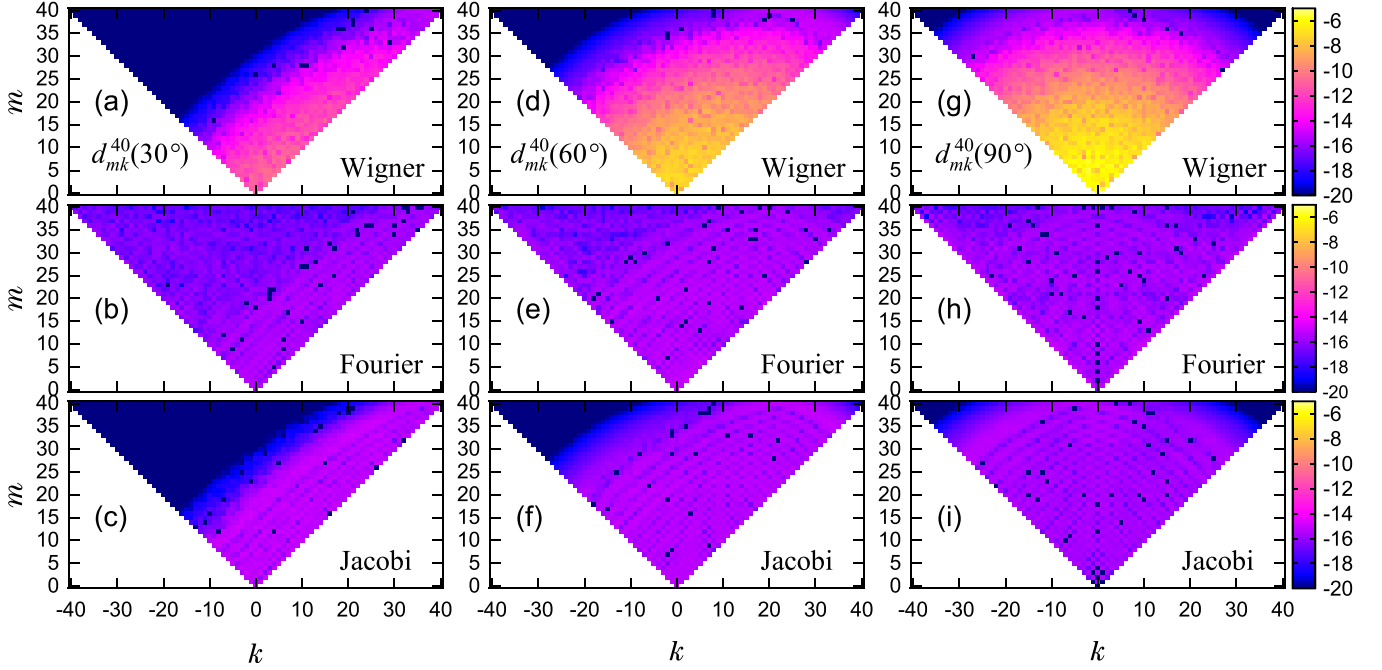


FIG. 3. The common logarithm of the error in the numerical value of the d function, i.e., $\log_{10}|\text{error}|$ of $d_{mk}^j(\theta)$, for different values of m and k , with $j = 40$, $\theta = 30^\circ$, 60° , and 90° . The results of the Jacobi algorithm are compared with those of the Wigner and Fourier methods. See the text for details.

$$d_{mk}^j(\theta) = d_{-k-m}^j(\theta), \quad (15c)$$

$$d_{mk}^j(-\theta) = (-1)^{m-k} d_{mk}^j(\theta), \quad (15d)$$

$$d_{mk}^j(-\theta) = d_{km}^j(\theta), \quad (15e)$$

$$d_{mk}^j(\pi - \theta) = (-1)^{j+m} d_{m-k}^j(\theta). \quad (15f)$$

It can be seen from Fig. 2 that the maximum error from the Wigner method increases exponentially with j , in the way similar as that of W_n^{jmk} in Eq. (3) of the Wigner formula. Already when $j \geq 25$ the error would exceed 10^{-10} , which may lead to serious numerical problems in applications such as high-spin calculations in nuclear physics. The origin for

loss of precision in the Wigner method is clear. It is caused by the summation over many W_n^{jmk} terms in Eq. (3), where numerical errors are accumulated following a power law of j .

On the contrary, the maximum error from the Fourier method keeps almost constant in a stable way towards high spins, with the precision as high as about 10^{-14} even when $j \approx 100$. Although the Fourier method in Eq. (7) also involves a summation over many terms, each term has very high precision since the corresponding Fourier coefficient t_ρ^{jmk} is calculated by means of the formula-manipulation software MAXIMA with very high precision and is stored into a memory [3], so that the accumulation of numerical errors can be avoided.

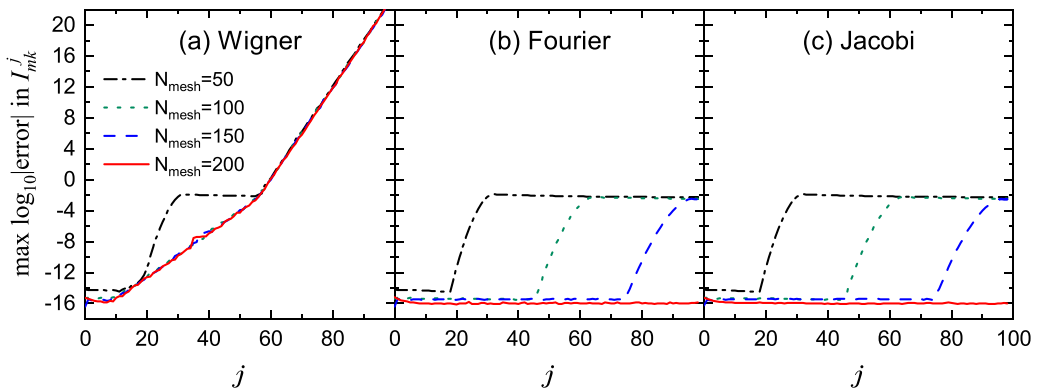


FIG. 4. The common logarithm of the maximum error in the numerical value of the integral I_{mk}^j in Eq. (18) by the Gauss-Legendre quadrature formula as a function of j . Cases with different number of mesh points N_{mesh} by the Jacobi algorithm are compared with those of the Wigner and Fourier methods. The maximum error is taken over all the possible values of m and k for each j . See the text for details.

For the Jacobi method, as seen from Eq. (10), there is no summation over many terms with large numbers and a high-precision evaluation of the d function is then expected. As seen from Fig. 2, when the Jacobi polynomial is calculated directly by its expression of Eq. (12), a very similar loss of precision is found for the Jacobi method as the Wigner formula. This is due to the fact that Eq. (12) involves summation over terms that include factorials of large numbers, which leads to accumulation of numerical errors. However, when the recurrence relations of the Jacobi polynomial in Eqs. (13), (14) are adopted, the Jacobi method provides a similar high-precision and stable behavior of the d function as the Fourier method. This clearly suggests that it is the recurrence relations in Eqs. (13), (14) that avoid accumulation of numerical errors. Using the recurrence relations to improve numerical precision may be helpful for many other numerical problems. Hereafter, the Jacobi method with the recurrence relations in Eqs. (13), (14) is referred to as the Jacobi algorithm for the d -function evaluation.

To further carry out precision analysis in details, we take the $j = 40$ case as an example and show in Fig. 3 errors of $d_{mk}^{40}(\theta)$ for different values of m, k , and θ , with $\theta = 30^\circ, 60^\circ, 90^\circ$, and $0 \leq m \leq j, k \leq |m|$ due to the symmetries in Eq. (15). The results of the Jacobi algorithm (with the recurrence relations) are compared with those of the Wigner and Fourier methods. It is seen that the Fourier method gives uniformly a 10^{-14} – 10^{-15} precision nearly irrespective of m, k , and θ . The Wigner method, however, leads to a rather unstable precision, depending sensitively on m, k , and θ . The precision from the Wigner method could have errors as large as $\approx 10^{-5}$ when $m \sim k \sim 0$ and $\theta = 90^\circ$ as seen from Fig. 3(g), or it could be very accurate, with the precision as high as 10^{-20} when $m \sim j, k \sim -j, \theta = 30^\circ$ and 60° [see Fig. 3(a) and (d)] or $m \sim j, |k| \sim j, \theta = 90^\circ$ [see Fig. 3(g)], which, for these special cases, is much better than the Fourier method.

Therefore, In Ref. [3], Tajima suggested that if a very high precision is needed for the d -function evaluation, one should develop a program to switch between the Wigner and Fourier methods with special values of j, m, k , and θ . It is now very interesting to compare the results of the Jacobi algorithm (with the recurrence relations) in Fig. 3. For each set of j, m, k , and θ , the Jacobi algorithm always reproduces the one with the higher precision between the Wigner and Fourier methods. This pleasant feature in the Jacobi algorithm makes it a natural choice for a switcher as discussed in Ref. [3].

IV. ERROR ANALYSIS WHEN THE WIGNER d FUNCTION IS INTEGRATED

According to the Peter-Weyl theorem, the Wigner D functions, $D_{mk}^j(\phi, \theta, \psi)$, form a complete set of orthogonal functions of the Euler angles, and are often used to expand functions that are related to rotation. As the Euler angles are continuous variables the expansion takes the form of integrals with $D_{mk}^j(\phi, \theta, \psi)$ being part of the integrand. Because of the highly oscillatory behavior of the d function, as shown in Fig. 1, especially at high j 's, a high precision in numerical calculations for integrals involving the d function becomes an issue.

For discussions, let us take an example from the calculation with angular-momentum projection for the symmetry-violated nuclear wave functions from mean-field calculations. Assuming axial symmetry for the intrinsic states, $|\Phi_\kappa\rangle$, the d function enters into the calculation through the angular-momentum projector,

$$\hat{P}_{mk}^j = \left(j + \frac{1}{2}\right) \int_0^\pi d_{mk}^j(\theta) \hat{R}(\theta) \sin \theta d\theta, \quad (16)$$

where $\hat{R}(\theta) = e^{-i\theta \hat{j}_y}$ is the rotation operator around the y axis. It can be generally shown [10] that the calculated Hamiltonian and Norm projected matrix elements, for example, take the form

$$\begin{aligned} H_{kk'k''}^j &= \left(j + \frac{1}{2}\right) \int_0^\pi d_{kk'}^j(\theta) \langle \Phi_\kappa | \hat{H} \hat{R}(\theta) | \Phi_{\kappa'} \rangle \sin \theta d\theta, \\ N_{kk'k''}^j &= \left(j + \frac{1}{2}\right) \int_0^\pi d_{kk'}^j(\theta) \langle \Phi_\kappa | \hat{R}(\theta) | \Phi_{\kappa'} \rangle \sin \theta d\theta, \end{aligned} \quad (17)$$

which is an integral over the Euler angle θ with essentially two kinds of functions in the integrand, $d_{kk'}^j(\theta)$ and the rotated matrix elements $\langle \Phi_\kappa | \hat{O} \hat{R}(\theta) | \Phi_{\kappa'} \rangle$ with $\hat{O} = \hat{H}$ or 1, which is expected to be a smooth function of θ . Due to the highly oscillatory behavior of the d function, its precision may be more important for integrals involving the d function as in many potential applications in nuclear physics, quantum metrology and many other fields in the future.

First, in Fig. 4 we take one such integral for discussions and show the absolute value (error) of the following integral:

$$I_{mk}^j = \int_0^\pi d\theta \sin \theta d_{mk}^j(\theta) d_{mk}^{j+1}(\theta) = 0 \quad (18)$$

calculated by the standard Gauss-Legendre quadrature formula with different number of mesh points N_{mesh} . The results of the Jacobi algorithm are compared with those of the Wigner and Fourier methods. It is seen that the error from the Wigner method increases rapidly with j and exceeds 10^{-8} at $j \gtrsim 35$, irrespective of N_{mesh} , indicating that the error comes mainly from the d function. By comparison, the error from the Jacobi algorithm and Fourier method depends on N_{mesh} and the precision of the integral (18) could be as high as 10^{-16} for $j \leq 100$ if $N_{\text{mesh}} = 200$ is taken. This suggests that the Jacobi algorithm for the d function applied in integration calculations can achieve a similar high precision as the Fourier method. The remaining errors in Fig. 4 should then come mainly from the quadrature formula.

Of course, in numerical calculations and practical applications much more complicated integrands generally appear in integrals, for which a large N_{mesh} is expected, and causes heavier computational burden. Nevertheless, the results in Fig. 4(b) and (c) suggest that one has a choice to use smaller numbers of mesh points if states of only lower angular momenta are studied.

V. A REALISTIC CALCULATION WITH DIFFERENT d -FUNCTION METHODS IN THE ANGULAR MOMENTUM PROJECTOR

Today's experimental measurements can provide data for very high-spin states. For example, along the yrast rotational band of ^{156}Dy , the measurement could reach spin states as high as $j = 62$ [47]. Physically, as a nucleus rotates faster and faster, the Coriolis antipairing effect [5] gradually breaks the nucleon pairs that are formed in the ground state. In the theoretical description by the projected shell model [10–12], states of broken-pairs can be explicitly included in the configuration space in terms of multi-quasiparticle (qp) states. Therefore, our discussion on the precision of the d function calculation should be coupled with the structure of multi-qp states.

We show next that the precise d function evaluation enables extension in realistic calculations for nuclear states in the high-spin region where the conventional Wigner method usually collapses due to numerical instability. In an angular-momentum-projection calculation, the kernel ingredients involve the Hamiltonian and norm matrix elements described in Eq. (17). Here, we take the diagonal elements of the norm matrix $N_{kk\,kk}^j$ for discussion, where k appears in the d function and κ labels the multi-qp state. Note that the norm matrix, which appears generally in all models with angular momentum projection, reflects purely a geometric structure of the projected states, and therefore, the following discussions do not depend on any specific model interactions.

In Fig. 5, we show $N_{kk\,kk}^j$ for different multi-qp states $|\Phi_\kappa\rangle$ for ^{156}Dy calculated by the projected shell model [10,20], with the Wigner d function obtained by our new Jacobi and the conventional Wigner algorithm. The multi-qp states include the qp vacuum (0-qp) state and other selected ones, each from the 2-qp, 4-qp, 6-qp, 8-qp, and 10-qp configurations. Keeping in mind that the physical meaning of $N_{kk\,kk}^j$ is the probability of finding angular momentum j in the corresponding intrinsic state, Fig. 5(a) actually shows the distribution of the j components in each intrinsic configuration. The general trend of the j distribution in each curve is such that after a local maximum at very low spins, the curve decays exponentially toward high spins. In the 0-qp state, for example, the content for $j = 42$ is as small as 10^{-9} . Figure 5(a) shows clearly that at very high spins, the higher-order qp states in the configuration space play more important roles in providing high- j components in the intrinsic states. Physically, these angular momenta are supplied by the broken-pair nucleons in the higher order qp configurations. In the 10-qp state, for example, the content for $j = 42$ becomes larger than 10^{-4} . The numerical results from the calculation with the Jacobi algorithm for d function are stable. The same stable results are obtained by calculations with the Fourier algorithm.

In contrast, due to the loss of precision in the Wigner algorithm for the d function as shown in Fig. 2, coupled with the fact of tiny contents of high angular momenta in the intrinsic states, the calculated $N_{kk\,kk}^j$ curves in Fig. 5(b) seem have terrible errors at high spins. The rather unphysical results indicate that the calculation breaks down completely, for example, for $j \gtrsim 42$ in the 0-qp state in our ^{156}Dy case. Although for the multi-qp states, errors occur later at some higher spins,

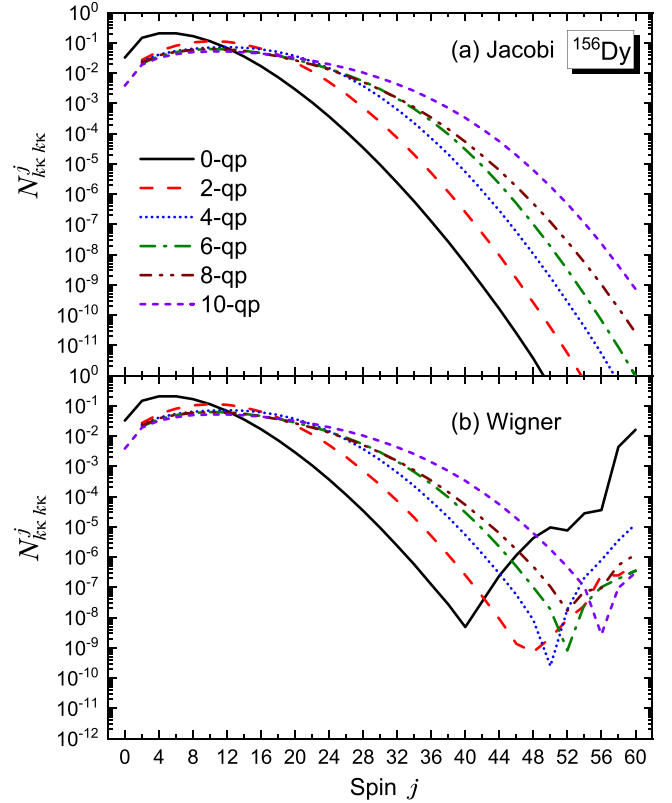


FIG. 5. The diagonal elements of the Norm matrix $N_{kk\,kk}^j$ of Eq. (17) for different multi-qp states $|\Phi_\kappa\rangle$ of ^{156}Dy calculated by using the Jacobi and Wigner algorithms for the d function. See the text for details.

the fatal error at $j = 42$ in the 0-qp state essentially stops the calculation for higher spin states. Figure 6 shows energies of the yrast band for ^{156}Dy as functions of j , calculated by the projected shell model [10,20] with the Wigner, Fourier, and Jacobi algorithms for the Wigner d function in the angular-momentum projector. The existing experimental data [47] are also shown for comparison. It is seen that with the Jacobi (as well as the Fourier) algorithm, the results excellently describe the data up to the highest spin with $j = 60$. On the contrary, the calculation with the conventional Wigner algorithm stops at $j = 42$, and gives unphysical results for $j \geq 44$. As in the projection calculation, the j -dependence of the rotational energies is entirely through the d function [see Eq. (17)], we conclude that the numerical errors in the results seen in Fig. 6 originate from the problem in the conventional Wigner algorithm.

VI. SUMMARY

To probe the extreme in angular momentum in nuclear physics, numerical calculations are required for very high-spin states. With the worldwide effort for building modern facilities and γ -ray detectors, it is anticipated that more and more high-spin data will be collected and the demand for precise high-spin calculations is increasing. The Wigner D (d) functions serve as indispensable ingredients for many

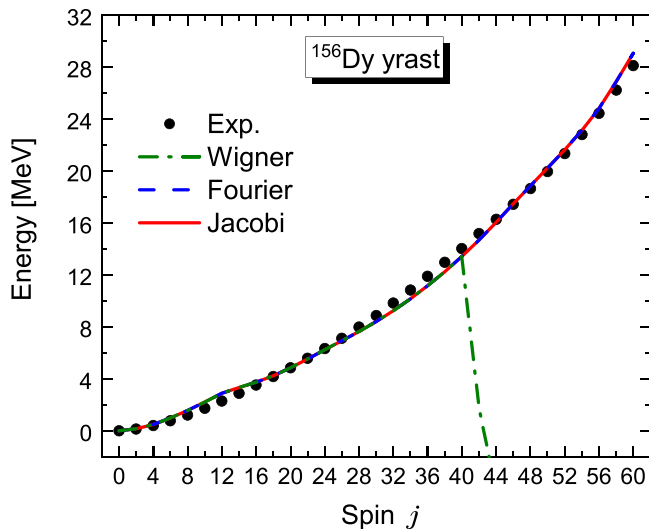


FIG. 6. The energies of the yrast band for ^{156}Dy calculated by the projected shell model [10,20] with three different algorithms for the d function in the angular-momentum projector. The results are compared with the experimental data taken from Ref. [47].

nuclear-structure models and are important for nuclear physics, quantum metrology, and many other fields. Numerical evaluation of the Wigner d function, $d_{mk}^j(\theta)$, from the conventional Wigner method suffers from serious errors and instability at medium and high spins. In this paper we present a high-precision and stable algorithm for evaluation of the Wigner d function. The algorithm is based on the Jacobi polynomial and its recurrence relations.

Compared with the conventional Wigner method, the loss of precision at medium and high spins is avoided in our Jacobi algorithm, with a very high precision 10^{-14} – 10^{-15} when $j \leq 100$. Compared with the recent Fourier method, our Jacobi algorithm avoids the dependence on formula-manipulation softwares and does not need a large memory. With the help from the recurrence relations of the Jacobi polynomial, the Jacobi algorithm always gives the best precision so far irrespective of the values of j, m, k , and θ . Furthermore, it is self-contained, and therefore, user-friendly.

The Jacobi algorithm could be the most effective algorithm for the Wigner d -function evaluation in nuclear physics, quantum metrology, and many other fields in the future. Through numerical proofs with a realistic example for the yrast band of ^{156}Dy , we have shown that with our proposed Jacobi algorithm, the calculation (as well as that by the Tajima Fourier algorithm) can be aggressively extended to the high-spin region where the conventional Wigner method breaks down completely. The related FORTRAN90 testing code and subroutines for the Wigner and Fourier methods as well as the Jacobi algorithm are provided as Supplemental Material [46] of the present article.

ACKNOWLEDGMENTS

L.J.W. would like to thank Prof. Z.-C. Gao for discussions and comments. This work is supported by the Fundamental Research Funds for the Central Universities (Grant No. SWU-KT22050), by the National Natural Science Foundation of China (Grants No. 12275225, No. 12235003, and No. U1932206), and partially supported by the Key Laboratory of Nuclear Data (China Institute of Atomic Energy).

- [1] M. Guidry and Y. Sun, *Symmetry, Broken Symmetry, and Topology in Modern Physics: A First Course* (Cambridge University Press, Cambridge, 2022).
- [2] D. A. Varshalovich, A. N. Moskalev, and V. K. Khersonskii, *Quantum Theory of Angular Momentum* (World Scientific, Singapore, 1988).
- [3] N. Tajima, Analytical formula for numerical evaluations of the Wigner rotation matrices at high spins, *Phys. Rev. C* **91**, 014320 (2015).
- [4] J. Suhonen, *From Nucleons to Nucleus* (Springer-Verlag, Berlin, 2007).
- [5] P. Ring and P. Schuck, *The Nuclear Many-Body Problem* (Springer-Verlag, Berlin, 1980).
- [6] L. Pezzé, A. Smerzi, G. Khoury, J. F. Hodelin, and D. Bouwmeester, Phase Detection at the Quantum Limit with Multiphoton Mach-Zehnder Interferometry, *Phys. Rev. Lett.* **99**, 223602 (2007).
- [7] L. Pezzé and A. Smerzi, Mach-Zehnder Interferometry at the Heisenberg Limit with Coherent and Squeezed-Vacuum Light, *Phys. Rev. Lett.* **100**, 073601 (2008).
- [8] T. Miyazaki, M. Katori, and N. Konno, Wigner formula of rotation matrices and quantum walks, *Phys. Rev. A* **76**, 012332 (2007).
- [9] L. P. Yang, Y. Li, and C. P. Sun, Franck-Condon effect in central spin system, *Eur. Phys. J. D* **66**, 300 (2012).
- [10] K. Hara and Y. Sun, Projected shell model and high-spin spectroscopy, *Int. J. Mod. Phys. E* **04**, 637 (1995).
- [11] Y. Sun and D. H. Feng, High spin spectroscopy with the projected shell model, *Phys. Rep.* **264**, 375 (1996).
- [12] Y. Sun, Projection techniques to approach the nuclear many-body problem, *Phys. Scr.* **91**, 043005 (2016).
- [13] T. Nikšić, Z. P. Li, D. Vretenar, L. Próchniak, J. Meng, and P. Ring, Beyond the relativistic mean-field approximation. III. Collective Hamiltonian in five dimensions, *Phys. Rev. C* **79**, 034303 (2009).
- [14] T. Nikšić, D. Vretenar, and P. Ring, Relativistic nuclear energy density functionals: Mean-field and beyond, *Prog. Part. Nucl. Phys.* **66**, 519 (2011).
- [15] J. L. Egido, State-of-the-art of beyond mean field theories with nuclear density functionals, *Phys. Scr.* **91**, 073003 (2016).
- [16] J. M. Yao, J. Meng, Y. F. Niu, and P. Ring, Beyond-mean-field approaches for nuclear neutrinoless double beta decay in the standard mechanism, *Prog. Part. Nucl. Phys.* **126**, 103965 (2022).
- [17] J. A. Sheikh, G. H. Bhat, Y.-X. Liu, F.-Q. Chen, and Y. Sun, Mixing of quasiparticle excitations and γ vibrations in transitional nuclei, *Phys. Rev. C* **84**, 054314 (2011).

- [18] P. W. Zhao, P. Ring, and J. Meng, Configuration interaction in symmetry-conserving covariant density functional theory, *Phys. Rev. C* **94**, 041301(R) (2016).
- [19] C. W. Johnson and K. D. O'Mara, Projection of angular momentum via linear algebra, *Phys. Rev. C* **96**, 064304 (2017).
- [20] L.-J. Wang, F.-Q. Chen, T. Mizusaki, M. Oi, and Y. Sun, Toward extremes of angular momentum: Application of the Pfaffian algorithm in realistic calculations, *Phys. Rev. C* **90**, 011303(R) (2014).
- [21] L.-J. Wang, Y. Sun, T. Mizusaki, M. Oi, and S. K. Ghorui, Reduction of collectivity at very high spins in ^{134}Nd : Expanding the projected-shell-model basis up to 10-quasiparticle states, *Phys. Rev. C* **93**, 034322 (2016).
- [22] L.-J. Wang, F.-Q. Chen, and Y. Sun, Basis-dependent measures and analysis uncertainties in nuclear chaoticity, *Phys. Lett. B* **808**, 135676 (2020).
- [23] S. Jehangir, G. H. Bhat, N. Rather, J. A. Sheikh, and R. Palit, Systematic study of near-yrast band structures in odd-mass $^{125-137}\text{Pr}$ and $^{127-139}\text{Pm}$ isotopes, *Phys. Rev. C* **104**, 044322 (2021).
- [24] F. S. Babra, S. Jehangir, R. Palit, S. Biswas, B. Das, S. Rajbanshi, G. H. Bhat, J. A. Sheikh, B. Das, P. Dey, U. Garg, M. S. R. Laskar, C. Palshetkar, S. Saha, L. P. Singh, and P. Singh, Investigation of the alignment mechanism and loss of collectivity in ^{135}Pm , *Phys. Rev. C* **103**, 014316 (2021).
- [25] S. Jehangir, G. H. Bhat, J. A. Sheikh, S. Frauendorf, W. Li, R. Palit, and N. Rather, Triaxial projected shell model study of γ -bands in atomic nuclei, *Eur. Phys. J. A* **57**, 308 (2021).
- [26] V. Rani, S. Singh, M. Rajput, P. Verma, A. Bharti, G. H. Bhat, and J. A. Sheikh, Quasiparticle structure of low-lying yrast energy levels and γ -bands in $^{164-174}\text{Hf}$ nuclei, *Eur. Phys. J. A* **57**, 274 (2021).
- [27] Z.-R. Chen and L.-J. Wang, Pfaffian formulation for matrix elements of three-body operators in multiple quasiparticle configurations, *Phys. Rev. C* **105**, 034342 (2022).
- [28] Z.-C. Gao, Y. Sun, and Y.-S. Chen, Shell model method for Gamow-Teller transitions in heavy, deformed nuclei, *Phys. Rev. C* **74**, 054303 (2006).
- [29] L.-J. Wang, Y. Sun, and S. K. Ghorui, Shell-model method for Gamow-Teller transitions in heavy deformed odd-mass nuclei, *Phys. Rev. C* **97**, 044302 (2018).
- [30] T. R. Rodríguez and G. Martínez-Pinedo, Energy Density Functional Study of Nuclear Matrix Elements for Neutrinoless $\beta\beta$ Decay, *Phys. Rev. Lett.* **105**, 252503 (2010).
- [31] J. M. Yao, L. S. Song, K. Hagino, P. Ring, and J. Meng, Systematic study of nuclear matrix elements in neutrinoless double- β decay with a beyond-mean-field covariant density functional theory, *Phys. Rev. C* **91**, 024316 (2015).
- [32] L.-J. Wang, J. Engel, and J. M. Yao, Quenching of nuclear matrix elements for $0\nu\beta\beta$ decay by chiral two-body currents, *Phys. Rev. C* **98**, 031301(R) (2018).
- [33] L. Tan, Y.-X. Liu, L.-J. Wang, Z. Li, and Y. Sun, A novel method for stellar electron-capture rates of excited nuclear states, *Phys. Lett. B* **805**, 135432 (2020).
- [34] L.-J. Wang, L. Tan, Z. Li, G. W. Misch, and Y. Sun, Urca Cooling in Neutron Star Crusts and Oceans: Effects of Nuclear Excitations, *Phys. Rev. Lett.* **127**, 172702 (2021).
- [35] L.-J. Wang, L. Tan, Z. Li, B. Gao, and Y. Sun, Description of ^{93}Nb stellar electron-capture rates by the projected shell model, *Phys. Rev. C* **104**, 064323 (2021).
- [36] G. F. Bertsch and L. M. Robledo, Decay widths at the scission point in nuclear fission, *Phys. Rev. C* **100**, 044606 (2019).
- [37] L. M. Robledo, T. R. Rodríguez, and R. R. Rodríguez-Guzmán, Mean field and beyond description of nuclear structure with the Gogny force: A review, *J. Phys. G: Nucl. Part. Phys.* **46**, 013001 (2019).
- [38] D. Regnier, M. Verrière, N. Dubray, and N. Schunck, Felix-1.0: A finite element solver for the time dependent generator coordinate method with the gaussian overlap approximation, *Comput. Phys. Commun.* **200**, 350 (2016).
- [39] D. Regnier, N. Dubray, M. Verrière, and N. Schunck, Felix-2.0: New version of the finite element solver for the time dependent generator coordinate method with the gaussian overlap approximation, *Comput. Phys. Commun.* **225**, 180 (2018).
- [40] D. Regnier, N. Dubray, and N. Schunck, From asymmetric to symmetric fission in the fermium isotopes within the time-dependent generator-coordinate-method formalism, *Phys. Rev. C* **99**, 024611 (2019).
- [41] X. M. Feng, P. Wang, W. Yang, and G. R. Jin, High-precision evaluation of Wigner's d matrix by exact diagonalization, *Phys. Rev. E* **92**, 043307 (2015).
- [42] C. H. Choi, J. Ivanić, M. S. Gordon, and K. Ruedenberg, Rapid and stable determination of rotation matrices between spherical harmonics by direct recursion, *J. Chem. Phys.* **111**, 8825 (1999).
- [43] H. Dachsel, Fast and accurate determination of the Wigner rotation matrices in the fast multipole method, *J. Chem. Phys.* **124**, 144115 (2006).
- [44] G. Prézeau and M. Reinecke, Algorithm for the evaluation of reduced Wigner matrices, *Astrophys. J. Suppl. Series* **190**, 267 (2010).
- [45] M. Abramowitz and I. A. Stegun, *Handbook of Mathematical Functions with Formulas, Graphs, and Mathematical Tables*, Vol. 55 (US Government Printing Office, Washington, D.C., 1964).
- [46] See Supplemental Material at <http://link.aps.org/supplemental/10.1103/PhysRevC.106.054320> for the related testing code and subroutines about the Wigner d function, from which all the results in figures of the paper could be obtained. Note that the Jacobi algorithm is improved by adopting a $n! = x_n \times 32768^{y_n}$ algorithm for factorials.
- [47] C. Reich, Nuclear data sheets for $A = 156$, *Nucl. Data Sheets* **113**, 2537 (2012).